Control of *Drosophila* wing and haltere development by the nuclear *vestigial* gene product

Jim A. Williams, John B. Bell,[1] and Sean B. Carroll[2]

Howard Hughes Medical Institute, Laboratory of Molecular Biology, University of Wisconsin–Madison, Madison, Wisconsin 53706 USA; [1]Department of Genetics, University of Alberta, Edmonton, Alberta, Canada T6G-2E9

The Dipteran flight appendages, the wings and halteres, develop from larval imaginal discs that also produce other sections of the second and third thoracic adult body segments. Loss of *vestigial* (*vg*) function in *Drosophila* selectively eliminates wing and haltere formation. Here, we show that *vg* expression is spatially restricted to the presumptive wing and haltere regions of these imaginal discs. An intronic regulatory element mediates this restriction and may elaborate upon cues that activate *vg* expression in the embryonic disc primordia. The nuclear *vg* protein lacks any recognized nucleic acid-binding motif but is comprised of two putative functional domains, one of which bears similarity to part of the *Deformed* homeotic protein and may mediate protein–protein interactions. These results suggest that *vg* is directly involved in determining which thoracic imaginal disc cells will form wings and halteres, perhaps by interacting with other nuclear regulatory proteins.

[*Key Words*: *vestigial*; imaginal discs; pattern formation; *Deformed*; transvection; enhancer]

Received September 13, 1991; revised version accepted October 10, 1991.

Embryonic pattern formation in *Drosophila* has been the subject of extensive study, which has led to the identification of many key genes involved in establishing the larval body plan (for review, see Akam 1987; Ingham 1988; Scott and Carroll 1989). However, relatively little is known about the genes and processes that regulate the development of the adult fly. Cephalic and thoracic adult *Drosophila* structures are formed from segmentally restricted infoldings of the larval epidermis, called imaginal discs. Fate map analysis has shown that these cells are set aside from presumptive larval cells shortly after the blastoderm stage of embryonic development (Wieschaus and Gehring 1976a,b). Clonal analysis indicates that these cells proliferate until mid-embryogenesis (~12 hr of development; Madhaven and Schneiderman 1977), and by the end of embryogenesis they are visible as pouches of cells (20–70 cells each) associated with or invaginated from the larval epidermis (Madhaven and Schneiderman 1977). Proliferation resumes during the first larval instar (Madhaven and Schneiderman 1977), and by late larval development each disc contains several thousand cells (53,000 cells in the wing disc; Whittle 1990). During metamorphosis, these pouches evaginate to form the adult cuticle (i.e., the epidermal structures of the head and thorax, and all adult appendages).

The two sets of Dipteran flight appendages, the wings and halteres, develop from the wing and haltere imaginal discs, respectively. However, these discs are also responsible for the formation of a variety of other adult cuticular structures. The wing disc forms virtually all of the cuticular structures of the adult thoracic cuticle (i.e., the notum), whereas the haltere disc forms parts of the thoracic postnotum cuticle. The intricate pattern of bristles on the adult thoracic cuticle and analysis of mutants that alter this pattern imply that complex positional information exists in these discs. This is reflected by the fact that a variety of enhancer trap lines show complex spatially restricted patterns of expression in imaginal discs (for review, see Whittle 1990; Wilkins and Gubb 1991). Mosaic analysis has shown that much of this positional information is established during larval development (Garcia-Bellido 1975) and relies largely on cell–cell interactions (Bryant et al. 1981; Whittle 1990; Wilkins and Gubb 1991).

The analysis of genes required for specific aspects of pattern formation within these discs should allow a dissection of the mechanisms by which pattern is established in these discs. The *vestigial* (*vg*) gene is a good candidate gene for this type of analysis. The *vg* product is required in a variety of tissues during morphogenesis and is also required during late larval development (the third-larval instar) primarily for formation of specific regions of the wing and haltere imaginal discs (Stanley 1931; Fristrom 1969; Bownes and Roberts 1981). *vg* mutants undergo extensive cell death in the presumptive wing

[2]Corresponding author.

region of third-larval instar imaginal wing discs (Fristrom 1969; Bownes and Roberts 1981), which results in the observed complete elimination of wing structures in homozygous *vg* adults. Cell death is a consequence of a cell-autonomous inability of *vg* discs to differentiate the presumptive wing region of the larval wing disc (Bownes and Roberts 1981). Presumably, a similar defect occurs in the haltere disc, because haltere derivatives of this disc are specifically deleted in *vg* mutants. Thus, analysis of *vg* function and regulation may provide clues to help understand aspects of both wing and haltere development as well as pattern formation in imaginal discs.

Here, we report a detailed study of the *vg* locus, the presentation of which is organized into two parts. The first describes the regulation and expression of the *vg* gene, and the second part investigates the structure and function of the *vg* product. *vg* is expressed in the embryonic wing and haltere imaginal disc precursors, from the extended germ-band stage through hatching. In late larvae, *vg* is expressed in a spatially restricted pattern identifying the subregions of these discs that will form wings and halteres (and require *vg* function). An intronic regulatory element required for this larval wing region expression is characterized and shown to be interspecifically conserved. We demonstrate that the *vg* protein is localized to the nuclei of cells fated to form wing and haltere derivatives. We have determined the primary sequence of the *vg* protein, which appears to be modular in structure, containing at least two putative functional domains. One of these domains contains two paired repeats and homology to a region of the *Deformed* homeotic protein. This domain may mediate protein–protein interactions with other nuclear regulatory proteins involved in wing and haltere specification.

Results

The phenotype of an adult null *vg* allele is shown in Figure 1b. Wing and haltere structures are eliminated completely, owing to extensive cell death in these regions of the larval imaginal discs. The fly also shows a number of other defects (e.g., erect postscuttellar bristles and reduced size), owing to a requirement for *vg* function during morphogenesis (Williams and Bell 1988). The regulatory mutant vg^{83b27} exhibits the same loss of wing and haltere functions (Fig. 1c) but none of these other pleiotropic effects (see below).

The *vg* locus has been cloned (Williams and Bell 1988), and a single 3.8-kb *vg* transcript has been identified. The isolation of several *vg* cDNAs and the generation of a crude exon map based on restriction endonuclease and Southern blot hybridization analyses have been reported (Williams et al. 1990a), and these data are summarized in Figure 1d.

The vg *transcript is expressed in the embryonic and larval wing and haltere imaginal discs*

We have determined the expression pattern of *vg* mRNA in wholemount embryos and imaginal discs utilizing digoxygenin-labeled cDNA probes (see Materials and methods). Extensive proteinase K treatment was required to detect embryonic *vg* transcripts, as a result of their very low abundance (Williams et al. 1990a). *vg* expression is first detected in germ-band-extended embryos (stage 10) in lateral stripes from the first thoracic (T1) to the seventh abdominal (A7) segments (Fig. 2a). By late germ-band extension (stage 11), three additional ventrolateral clusters of cells in T1–T3 also express *vg* (Fig. 2b). By following the fate of the T2 and T3 clusters through the remainder of embryonic development, we conclude that most or all of these cells correspond to the embryonic primordia of the wing and haltere discs (see below). The T1 cluster is seen only during this stage and later germ-band retraction stages and is not detected reproducibly at later stages. This cluster may correspond to the dorsal prothoracic disc primordia.

During germ-band retraction (stage 12), segmentally repeated expression is also detected in discrete cells in the ventral nerve cord (Fig. 2c). By the beginning of dorsal closure (stage 13), additional head region and ventral nerve cord cells express *vg*, and the ventrolateral clusters (wing and haltere disc primordia) begin to migrate dorsally (data not shown). During the early stages of head involution (stage 14), the pattern of expression is quite complex (Fig. 2d). The ventrolateral clusters are clearly visible as discrete pockets of cells, located laterally in T2 and T3 (Fig. 2d). These clusters correspond in location to the wing and haltere primordia, which have been detected at this stage using either fascillin III antibody staining (Bate and Martinez-Arias 1991) or whole-mount in situ hybridization with cDNA clones from the *Abnormal leg pattern* gene (Cohen et al. 1991). Groups of ventrolateral cells expressing *vg* mRNA flank the *vg*-positive ventral nerve cord cells (Fig. 2d). The lateral stripes from earlier stages have migrated dorsally, and clusters of cells in the head and abdominal regions express *vg* (data not shown). These structures may represent progenitors of sense organs of the peripheral nervous system. If *vg* protein is required in these cells, its function may be subtle or redundant, because no embryonic *vg* function has been reported. However, because the majority of embryonic *vg*-expressing cells may correspond to nervous system structures, loss of *vg* function could result in minor sensory defects. By the end of dorsal closure (stage 16) the complex *vg* pattern of expression begins to degenerate, and only the imaginal disc and ventral nerve cord expression persists until the end of embryogenesis (Fig. 2e). The wing and haltere discs can be seen clearly as lateral in-pockets of cells in stage 17 embryos (Fig. 2e,f). These correspond in size and location with the wing and haltere discs identified morphologically by Madhaven and Schneiderman (1977). It is of interest to note that the locations of the wing and haltere disc primordia at germ-band extension are very close to the respective locations of the meso- and metathoracic leg disc primordia (Cohen 1990). This is consistent with mosaic analysis, which has demonstrated that these pairs of primordia are closely positioned in the embryo (Wieschaus and Gehring 1976a).

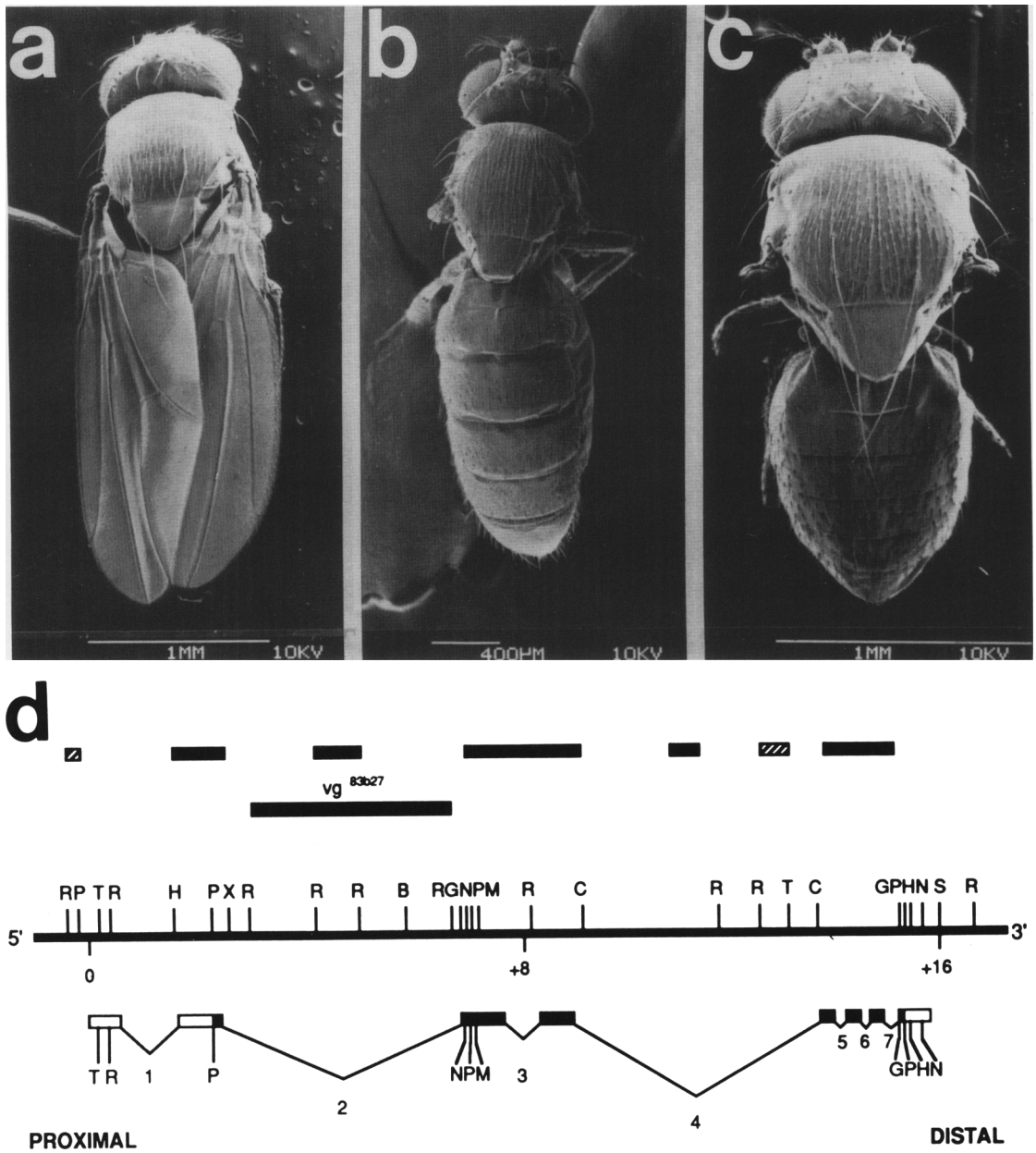

Figure 1. Function and organization of the *vg* locus. (*a*) An adult wild-type fly; (*b*) a homozygous null *vg* fly; (*c*) a homozygous vg^{83b27} fly. Note that the vg^{83b27} and *vg* homozygotes lack wings and halteres. (*d*) A partial restriction map of the *vg* locus, with *Cla*I (C); *Pst*I (P); *Hin*dIII (H); *Hin*cII (N); *Sal*I (S); *Sst*I (T); *Bgl*II (G); *Eco*R1 (R); and *Sma*I (M). An exon map of the *vg* transcription unit is also presented (*bottom*) (introns numbered), with relevant restriction sites indicated. The shaded region of the cDNA corresponds to the coding region. The deletion associated with the vg^{83b27} allele is denoted by a solid bar immediately *above* the map. Bars at the *top* denote regions of strong (solid) or weak (hatched) interspecific conservation of *vg* gene fragments between *D. melanogaster* and *D. virilis*, respectively.

In third-instar imaginal discs, *vg* expression is also limited to the wing and haltere discs and is expressed throughout these discs at very low levels (data not shown). However, *vg* is expressed at elevated levels in a broad stripe across these discs (Fig. 3a,b). In the wing disc, the zone of maximal expression includes the primordia for the wing pouch and hinge regions, which are deleted or altered in *vg* mutants (Bownes and Roberts 1981; James and Bryant 1981; Williams et al. 1990a). Expression in the haltere disc mimics that of the wing disc (Fig. 3b) and includes the primordia for the haltere structures, which are removed in *vg* mutants. Given that temperature-shift studies indicate a requirement for *vg* function during the third-larval instar (Stanley 1931) and the direct observation that loss-of-function *vg* mutants undergo cell death in this region of the disc during third-

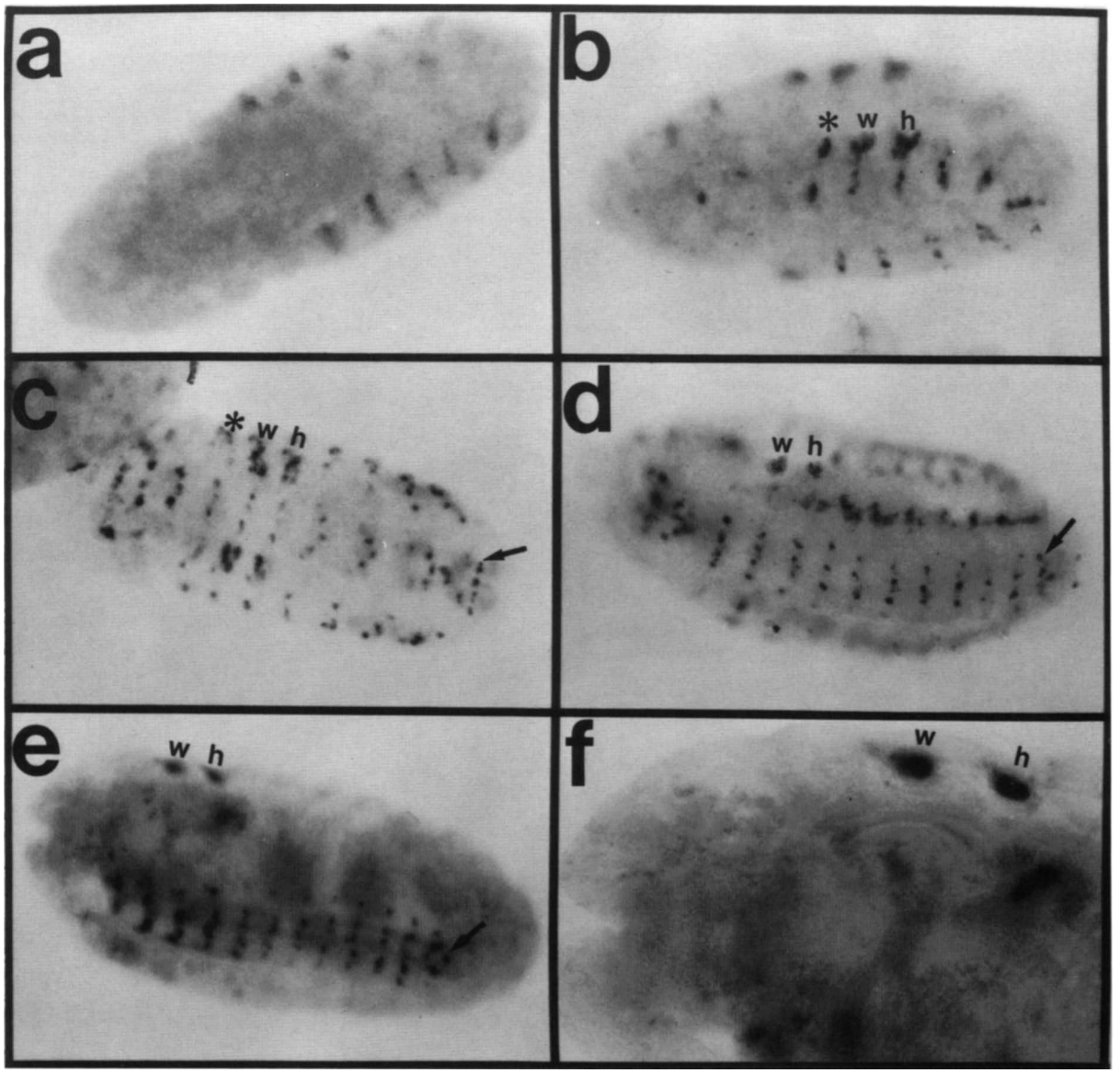

Figure 2. *vg* mRNA expression during embryonic development. The *vg* expression pattern in embryos was determined utilizing digoxygenin-labeled cDNA probes (see Materials and methods). A ventral orientation of a germ-band-extended embryo is shown in *a*; a later stage germ-band-extended embryo is shown in *b*. The T2 and T3 ventrolateral clusters (wing and haltere imaginal disc primordia) are labeled w (wing) and h (haltere) throughout. The transient T1 (*) cluster may correspond to the primordia of the dorsal prothoracic imaginal disc. A ventral view of a germ-band-retracting (stage 12) embryo is displayed in *c*; *d* shows a ventral view of a stage 14 dorsal-closure embryo. A stage 17 embryo is shown in *e*, with *f* depicting a high-magnification photo of the same embryo. All embryonic stages are as in Campos-Ortega and Hartenstein (1985). The ventral nerve cord expression is indicated with an arrow.

instar development (Fristrom 1969; Bownes and Roberts 1981; James and Bryant 1981), we conclude that the detected high-level expression is essential for wing and haltere formation.

The vg^{83b27} *allele deletes an intronic regulatory element required for gene expression in the wing and haltere imaginal discs*

Flies homozygous for the unusual recessive vg^{83b27} allele show extreme wing and haltere reductions but are wild type for all other *vg* phenotypes (see Fig. 1c). Molecular analysis reveals that vg^{83b27} deletes most of intron 2 (see Fig. 1d), indicating that sequences within intron 2 are somehow essential for wing and haltere development. It is unlikely that an alternatively spliced exon exists within this intron, as no candidate cDNAs have been identified in extensive screens of imaginal disc cDNA libraries (J. Williams, unpubl.). Because vg^{83b27} homozygotes exhibit only the wing and haltere phenotypes, it is more likely that the vg^{83b27} deletion has removed a con-

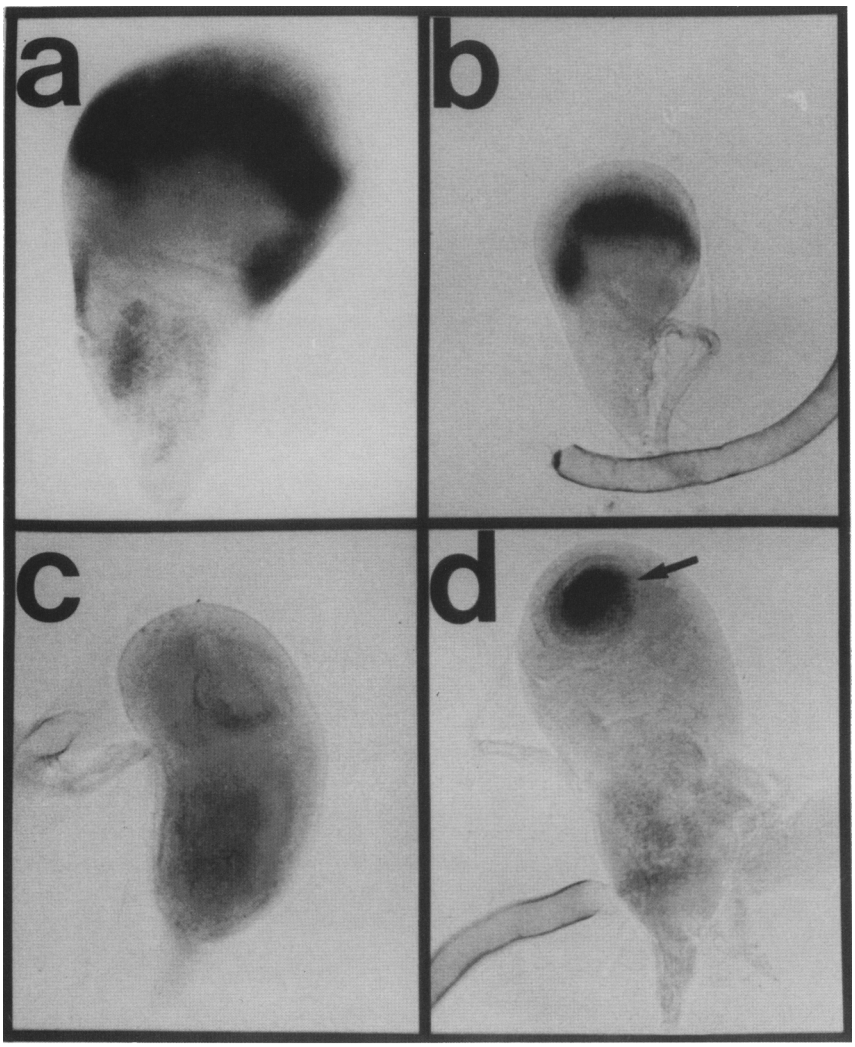

Figure 3. *vg* expression pattern in wild-type and vg^{83b27} wing and haltere imaginal discs. Digoxygenin in situ hybridization (see Materials and methods) was performed with either wild-type (*ab*) or vg^{83b27} imaginal disc complexes (*c,d*). The *vg* expression pattern in a wild-type wing disc and a wild-type haltere disc are shown in *a* and *b*, respectively. The *vg* expression pattern in two vg^{83b27} wing discs is shown in *c* and *d*. These discs are unusually narrow as a result of deletion of the entire wing pouch region of the disc (during the third-larval instar) in strong *vg* alleles (Bownes and Roberts 1981). Occasional discs exhibit a small part of the normal *vg* expression pattern (arrow in *d*), probably accounting for the observation that some vg^{83b27} flies have partial wing structures formed (Williams et al. 1990a). All discs are shown at the same level of magnification.

trol element that is required specifically for *vg* expression in these imaginal discs. To test this idea, the *vg* expression pattern in vg^{83b27} embryos and discs was determined (see Materials and methods). No alteration of *vg* expression was detected in vg^{83b27} embryos (data not shown). Thus, vg^{83b27} has not deleted sequences required for initial establishment of *vg* expression in the wing and haltere primordia (or for *vg* expression in the developing nervous system, etc.). In third-instar imaginal discs, faint expression is seen throughout the wing and haltere discs (data not shown). However, the elevated expression pattern detected in wild-type discs is absent in all vg^{83b27} discs examined (Fig. 3c). Thus, vg^{83b27} has deleted a control element required for region-specific amplification of *vg* expression in the wing and haltere discs during larval development. The loss of this high-level expression correlates with the loss of the wing pouch and part of the presumptive hinge region of the wing disc in vg^{83b27} (Fig. 3c), consistent with the prediction that this elevated expression is essential for wing development (see above). The fact that occasional discs exhibit a small part of the normal *vg* expression pattern (Fig. 3d) implies both that some additional regulatory sequences exist that have not been deleted and that the control element is complex.

The intronic regulatory element can mediate both cis- *and* trans-*activation of the* vg *promoter*

The vg^{83b27} allele complements recessive viable *vg* alleles genetically and partially complements some recessive lethal alleles (Alexandrov and Alexandrova 1987; Williams et al. 1990a). Because vg^{83b27} has deleted *vg* control sequences, it appears likely that the complementation is the result of alleles in *trans* to vg^{83b27} that retain a functional disc enhancer transmitting this information to the vg^{83b27} promoter via chromosome pairing (transvection; Lewis 1954). This would account for the ability of vg^{83b27} to complement all tested recessive viable *vg* alleles (Williams et al. 1990a), as these alleles are cytologically normal and do not alter the intronic region deleted in vg^{83b27} (Williams et al. 1990a). Several recessive null *vg* alleles have also been identified, on the basis of the phenotypes of these alleles when in *trans* to each

other or in *trans* to Df(2R)vg^B (vg^B), a cytologically visible deficiency of the *vg* locus (Williams and Bell 1988; Williams et al. 1990a,b). To test the prediction that chromosome pairing is required for complementation, the wing phenotype of flies containing these alleles in *trans* to vg^{83b27} was determined (for the origins and locations of the lesions associated with these alleles, see Materials and methods). Partial complementation is exhibited (i.e., wing and haltere phenotypes are significantly less extreme than either parent) when vg^{83b27} is heterozygous with vg^{nw} and vg^{12}, consistent with the fact that these are cytologically normal alleles that do not alter intron 2. Interestingly, no complementation is seen with vg^{136} or with the $vg^{WR2\text{-}4}$ alleles, all of which are associated with inversion breakpoints in either intron 1 or 2. These results argue that chromosome pairing is required for vg^{83b27} complementation, as these inversion breaks should disrupt chromosome pairing in this region.

Interspecific comparison of Drosophila melanogaster *and* Drosophila virilis vg *gene sequences identifies a potential conserved intronic control region*

The *Drosophila melanogaster* and *Drosophila virilis* lines diverged ~60 million years ago (Beverly and Wilson 1984). Previous comparisons of genes in these two species revealed that essential regions (i.e., conserved coding regions) have diverged ~10%, whereas nonfunctional sequences (i.e., some intronic regions) have diverged completely (Blackman and Meselson 1986; Kassis et al. 1986). Thus, functional regions within genes can be identified, on the basis of the degree of DNA sequence conservation between the cognate genes in the two species.

We have cloned the *D. virilis vg* locus and used Southern hybridization analyses to identify conserved regions within the *vg* loci (see Materials and methods). The locations of the strongest hybridizing restriction fragments detected in this analysis are shown in Figure 1d. As expected, several of these regions correspond to coding exons of the *vg* transcription unit (see below). The primarily noncoding exons 1 and 2 and the 3′-untranslated region are not as heavily conserved. However, the high AT content of these regions (see below) may obscure the detection of conserved sequences, owing to the low melting point of AT-rich hybrids. In addition, four nonexonic conserved restriction fragments were also identified (see Fig. 1). One strongly conserved region was detected in intron 2 and is the only conserved region detected within the region deleted in vg^{83b27} (Fig. 1). The conserved *D. melanogaster* intron 2 restriction fragment was used to probe Southern blots of DNA fragments of the *D. virilis* locus; this localized the homologous region in *D. virilis* to a small restriction fragment in approximately the same location as in the *D. melanogaster* gene (data not shown). Both regions were sequenced, and alignment revealed that a region of remarkable conservation (134 to 136 bp aligned) is present, which includes a 118-bp region of perfect conservation (J. Williams, unpubl.). This region is incapable of forming strong secondary structures and does not show significant homology (in either orientation) to any reported sequence (GenBank release 67 and EMBL release 26). To the best of our knowledge, this is the longest perfectly conserved region yet detected between *D. melanogaster* and *D. virilis*. Because it is likely that essential DNA would be evolutionarily conserved, this region is an excellent candidate for the location of an essential region of the intronic control element defined by the vg^{83b27} deletion.

vg *encodes a putative modular protein, with homology to the* Deformed *homeotic protein*

We have demonstrated that the *vg* transcript is expressed in a complex spatially restricted pattern in the embryo and that imaginal disc expression is restricted to subregions of the wing and haltere disc shown to require *vg* function. To further elucidate the potential function of the *vg* gene product, we have identified the predicted *vg*-coding sequence from cloned cDNAs. The nucleotide sequence of the longest cDNA (cDNA1), as well as corresponding genomic intervals, was determined (see Materials and methods) and is shown in Figure 4. The size of the transcript is 3.5 kb (without a poly(A) tail), in good agreement with size estimates from Northern analysis (3.7–3.8 kb). However, primer extension analysis will be required to precisely map the transcription start sites. A conceptual translation of the longest *vg* open reading frame (ORF) is shown above the sequence. The *vg* protein is predicted to be 453 amino acids long, with a molecular mass of 46 kD. Hydrophobicity analysis (not shown) indicates that no obvious signal peptide or strongly hydrophobic regions characteristic of transmembrane domains is present in the *vg* product. This implies a cell-internal role for the protein, consistent with immunolocalization studies (see below) and genetic evidence indicating that the *vg* product is cell autonomous (Bownes and Roberts 1981). The putative protein is rich in serine (15%), alanine (13.5%), glycine (13%), and histidine (9%) residues. The alanine and glycine residues are distributed nonrandomly, with an alanine-rich interval in exon 3 and glycine-rich regions in exons 3 and 4 (see Fig. 4). The glycine-rich regions are encoded by GGX nucleotide repeats. This nucleotide repeat (pen repeat) has been identified in a number of *Drosophila* transcripts (Wilde and Akam 1987) and often codes for polyglycine in proteins.

A weak *vg* allele (vg^{79d5}) is associated with a small deletion that removes the 5′ end of exon 3 (removing the polyalanine region of the exon), thus producing an internally deleted transcript (Williams et al. 1990a). Clearly, the 5′ end of exon 3 (including the polyalanine repeat) is not essential for *vg* function (as vg^{79d5} is a weak *vg* allele that is associated with only mild nicking of the wing margin). The protein regions flanking the exon 4 glycine repeat are probably functional, because strong protein sequence conservation between *D. melanogaster* and *D. virilis* is seen in the intervals flanking the exon 4 glycine-rich interval (Fig. 5a). However, the glycine-rich region shows poor interspecific sequence conservation (Fig. 5a). These results are consistent with the idea that

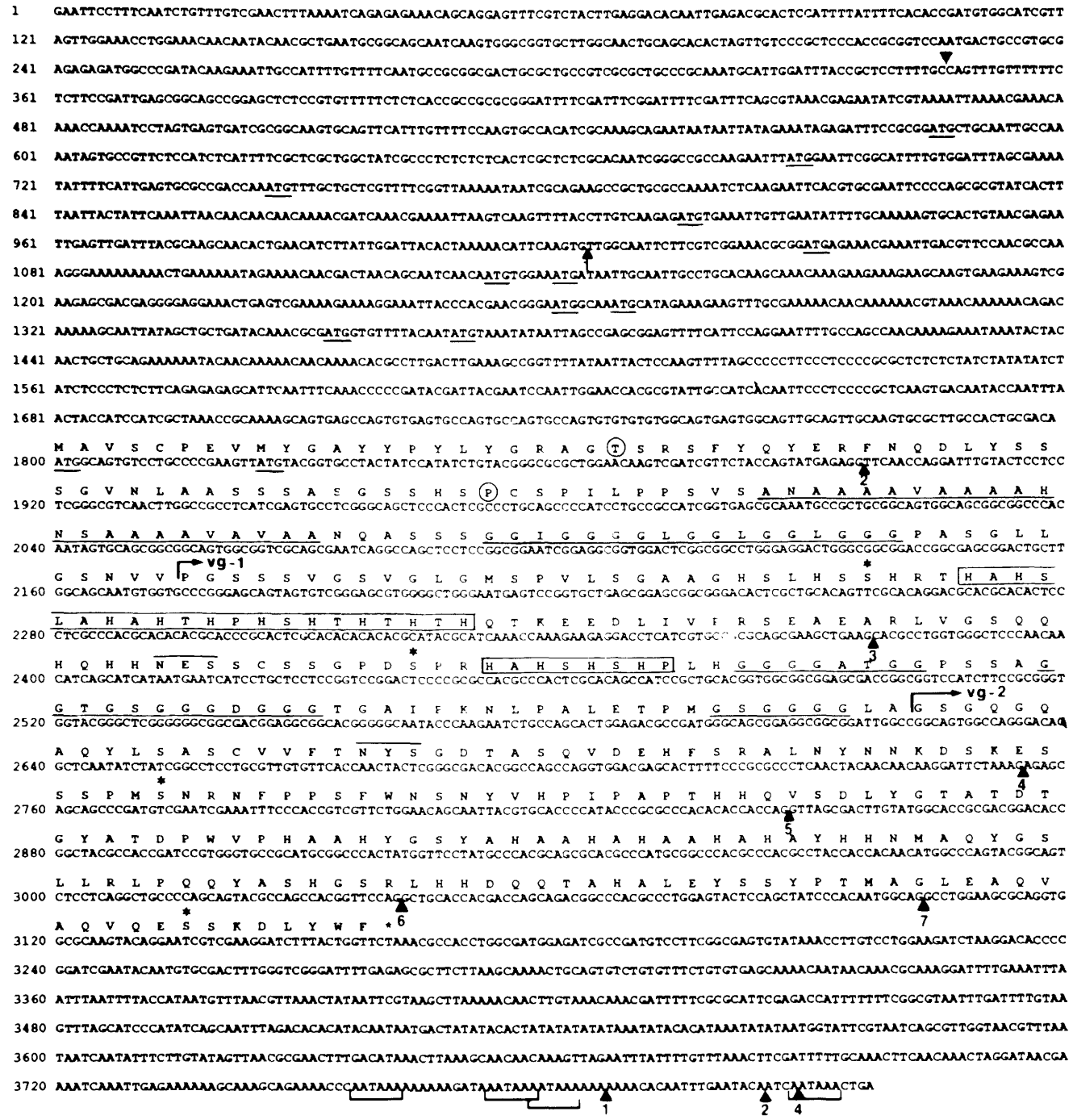

Figure 4. Sequence of the *vg* transcription unit. The sequence of the *vg* transcription unit and flanking genomic DNA is shown. The sequence begins at the *Eco*RI site at −0.4 kb (see Fig. 1). (▼) at bp 347 shows the 5′ extent of cDNA1. An additional 177 bp is present 5′ to this base in the cDNA. However, this DNA is derived from exon 2, probably as a consequence of aberrant cDNA synthesis. The numbered arrowheads below the sequence identify the intron junctions within the cDNA sequence; the numbered arrowheads at the *bottom* show the 3′ ends of cDNAs 1 (Williams et al. 1990a), 2, and 4. Four nongenomic A residues are present in cDNA2, demonstrating utilization of one of the upstream polyadenylation sites (AATAAA, in brackets) in this cDNA. A conceptual translation of the *vg* ORF is indicated *above* the sequence, with the alanine- or glycine-rich intervals underlined, as well as two potential N-linked glycosylation sites (NXS/T). The two *paired* repeats are boxed, and asterisks (*) indicate potential protein kinase C phosphoryation sites. The indicated ATG is probably utilized as the start codon, as this is the first ATG codon in the ORF and the sequence (GACAATG) shows strong homology to the translational consensus sequence (C/AAAA/CATG) reported in Cavener (1987). A 600-bp 3′-untranslated cDNA sequence follows the ORF. Four ATTTA and 11 ATTT sequences are present in this region. This may indicate that the *vg* transcript is rapidly degraded, as these sequences are associated with rapid turnover mRNAs (Shaw and Camen 1986). The ORF is preceded by an extremely long (at least 1453 bp) leader sequence containing 11 potential start codons (ATG; underlined), all of which have limited coding capacity (<44 amino acids in potential translatable length). The sequence shown is genomic DNA (Oregon-R). Of six detected coding-region polymorphisms, two result in amino acid substitutions (circled): threonine to proline (23) and proline to threonine (58). Labeled arrows correspond to the amino-terminal start sites of the *vg*-1 and *vg*-2 fusion proteins. Both clones extend to the *Bgl*II site 3′ to the stop codon.

Figure 5. Interspecific protein conservation and alignment of the *vg* and *Deformed* proteins. The predicted protein products of exon 4 from *D. melanogaster* and *D. virilis* are aligned in *a*. The respective amino acids are shown in the *top* and *bottom* lines, with dashes indicating gaps. Matched amino acids are indicated in the middle line, and double dots indicate conservative substitutions. The overall homology is only 65%. However, regions of high conservation are seen at both ends of the exon: 86% (30 of 35 amino acids) identity at the amino terminus and 85% (35 of 41 amino acids) conservation at the carboxyl terminus. The central glycine-rich interval (underlined) is highly diverged and difficult to align. The majority of the nucleotide alterations in the *D. virilis*-conserved regions result in silent site substitutions, consistent with the prediction that the product of this ORF is conserved. (*b*) The *vg* product (*top*) is aligned with the *Deformed* protein (*bottom*; Regulski et al. 1987). Amino acid coordinates within each protein are indicated, and glycine-rich intervals in the *vg* protein are underlined. The region of maximum homology is bracketed; potential N-linked glycosylation sites (NXS/T) are underlined. Amino acids identical in both proteins are shown between the sequences; double dots represent conservative substitutions. Dashes in the *Deformed* sequence denote gaps introduced to maximize the alignment. Both alignments were performed using the FASTA program (Pearson and Lipman 1988).

the *vg* homopolymeric repeats are not essential functional domains in the protein. It has been speculated that homopolymer repeats represent spacer intervals between functional domains in some proteins (Burtis et al. 1990). These observations suggest that the *vg* protein may be modular in structure, with a minimum of two functional domains linked by the exon 4 glycine-rich interval.

Data base searches revealed no significant homologies to the putative carboxy-terminal protein domain. However, two regions containing alternating histidine residues are present in the amino-terminal domain (see Fig. 4) and are similar to the previously characterized *paired* or His-Pro repeat (Frigerio et al. 1986). Although the function of this repeat is unknown, it has been identified in a number of *Drosophila* developmental genes, which include the *paired*, *bicoid* (Frigerio et al. 1986), *daughterless* (Cronmiller et al. 1988), *Deformed* (Regulski et al. 1987), and *E74* (Burtis et al. 1990) gene products. The *vg* and *Deformed* repeats are histidine alternating with predominately serine or threonine residues, whereas the *paired* gene repeat has a higher frequency of proline at these positions. The significance of this divergence is unknown. However, interspecific conservation analysis of the second *vg* repeat reveals that the alternating histidine residues in the repeat are perfectly conserved, whereas the identities of the alternative amino acids are flexible (Fig. 5a), implying that the observed divergence may not be functionally significant.

The *vg* sequence flanking and including both of these repeats is most similar to the *Deformed* protein (Fig. 5b). The region of maximum homology extends through a 109-amino-acid interval within *vg* exons 3 and 4, including essentially all of the putative *vg* amino-terminal domain. Within this interval, 33.7% identity is seen. If conservative substitutions are included (identified by the Fasta algorithm; Pearson and Lipman 1988), the level of amino acid similarity increases to 61%. Interestingly, the highest similarity is in the two alternating histidine repeats. The detected level of identity may be an overestimate of protein homology, because several gaps were introduced to maximize the alignments. However, the regions of conservation in both proteins (bracketed in Fig. 5b) show similar hydrophobicity profiles when compared to one another, and the conserved interval is near the amino terminus followed by a glycine-rich region in both proteins (not shown for *Deformed*). These results argue that *vg* and *Deformed* possess related protein domains, both of which contain two *paired* repeats organized in similar secondary structures. This domain appears essential for *vg* function, because the exon 4-encoded portion shows strong interspecific sequence conservation (Fig. 5a) and the exon 3 region is also strongly interspecifically conserved, as indicated by restriction fragment hybridization analysis (see Fig. 1).

The vg *protein is localized to cell nuclei and demarcates the wing- and haltere-forming subregions of these imaginal discs*

The *vg* product is required cell autonomously in the wing and haltere discs during the third-larval instar for formation of wing and haltere structures (Bownes and Roberts 1981). The regions of elevated *vg* expression in these discs include the structures deleted or altered in *vg* mutants. Thus, it is likely that the *vg* protein is required in these regions and is present at relatively high levels. A *vg*-specific antibody was generated (see Materials and methods) to test this possibility, as well as to determine the subcellular localization of the *vg* protein. The antibody-staining pattern corresponds to the mRNA expression pattern in embryos (data not shown) and in larval third-instar wing and haltere discs (Fig. 6a,b,d); high magnification (and double immunofluorescence labeling; see Materials and methods) shows that the *vg* protein is localized primarily in the nucleus (Fig. 6a). Comparison of the regions of *vg* protein expression with fate

maps of the wing and haltere discs (Bryant 1975) demonstrates that high-level *vg* expression marks most of the cells destined to form wing and hinge structures (and haltere structures in the haltere disc), but no (or low level) labeling is seen in the subregions of these discs that form notum or other thoracic cuticular structures (Fig. 6a). *vg* expression continues to mark wing structures, during the early and late stages of pupal wing eversion (Fig. 6, c and e, respectively), as well as everting haltere structures (data not shown). Thus, *vg* expression demarcates the presumptive wing- and haltere-forming regions of these imaginal discs, during both the determination and morphogenesis of these structures.

Discussion

The nuclear-localized vg *protein marks imaginal disc cells fated to form* Drosophila *flight appendages*

The *vg* gene is required to specify the identity of the presumptive wing region of the wing imaginal disc, and the corresponding region of the haltere disc. We have demonstrated that in larval imaginal discs, *vg* expression is limited to these discs and is expressed in the nuclei of cells that are fated to form wing and haltere structures.

Mutations in a number of *Drosophila* genes result in wing defects, including nicking, notching, or scalloping of the adult wing margin (Lindsley and Grell 1968). These genes are probably downstream of regulatory genes required specifically for wing formation, and their frequency reflects a requirement for a large number of gene products during wing formation. Only a small number of genes have been identified that when mutated, specifically eliminate all wing and haltere structures (but not other cuticular structures formed by these discs). This latter group of genes includes the *decapentapelegic* (*dpp*), *scalloped* (*sd*), *apterous* (*ap*), and *vg* genes; the genes likely encode factors that are globally required for *Drosophila* flight appendage formation. Of these genes, only the *ap*, *sd*, and *vg* genes appear to be required specifically for formation of wing and haltere structures, as they are not required for other pattern formation processes (Lindsley and Grell 1968; James and Bryant 1981). It is possible that these few genes have evolved to provide specific functions required for flight appendage formation. The *vg* gene is the only gene known to be expressed in the presumptive wing and haltere primordia, and we would argue that this pattern of gene expression, the strength of the *vg* phenotype, and the localization and structure of the *vg* gene product all support a fundamental role for *vg* in regulating flight appendage development.

The vg *protein may interact with other nuclear regulatory proteins*

What is the function of the *vg* protein in the developing wing and haltere? Analysis of the *vg* transcript indicates that the *vg* protein may have a modular structure and contains at least two putative functional domains linked by a glycine-rich interval. While neither domain is a known nucleic acid-binding motif, one domain is commonly found in DNA-binding proteins and shows similarity to part of the *Deformed* homeotic protein (a known DNA-binding protein). This domain contains two alternating histidine repeats (*paired* repeats) that are conserved in location and structure in both the *vg* and *Deformed* proteins. A similar repeat in the human high-molecular-weight kininogen protein has been shown to mediate protein–protein interactions with a negatively charged protein domain (see Haynes et al. 1989). These regions may interact with acidic domains in nuclear proteins that are regulated by or modulate *vg* and *Deformed* function. It has been observed that the *vg* and *Notch* genes interact synergistically (Rabinow and Birchler 1990), raising the possibility that *vg* may be a tissue-specific component of a cell interaction pathway required for formation of flight structures. If so, then *vg* may act, not as a direct DNA-binding protein, but by interacting with one or more other regulatory proteins to specify the wing and haltere modes of development, perhaps by regulating the expression of structural genes involved in cell differentiation and morphogenesis.

vg is clearly not the sole determinant required to promote wing differentiation, as loss of *vg* function results in cell death, rather than a transformation of wing-to-notum structures. It is likely that *vg* acts in parallel with several other genes (i.e., *ap*, *sd*) to promote flight appendage development. Loss of any one of these genes may result in an intermediate determinative state, in which the cells are unable to either form wing or return to the (potential) ground state of notum. This may result in the observed cell death seen in *vg* (as well as *ap* and *sd*) imaginal discs. If this is the case, it is possible that *vg* is tightly spatially regulated because high-level expression of *vg* elsewhere in the wing disc will cause abnormalities due to alterations to positional values within the disc. This possibility can be tested by examining the phenotypic consequences of ectopic expression of *vg*, by utilizing a P-element constuct that places a *vg* cDNA under heat shock control.

The larval imaginal disc expression pattern may require prior embryonic activation

During embryogenesis, low-level *vg* expression is established exclusively in the wing and haltere primordia and not in other identified disc primordia (i.e., leg or eye antennal disc primordia). It is of interest to speculate why *vg* expression is established early on in these disc primordia, as the *vg* protein is probably not required until later larval development (from temperature-shift analysis; Stanley 1931). It is possible that general low-level *vg* expression in these embryonic primordia is part of a two-step process required to set up the later high-level spatially restricted larval expression pattern. In the first step, expression is initiated in a subset of the embryonic imaginal disc primordia. In the second stage, region-specific amplification of expression occurs during larval development in these discs. This results in the final pattern

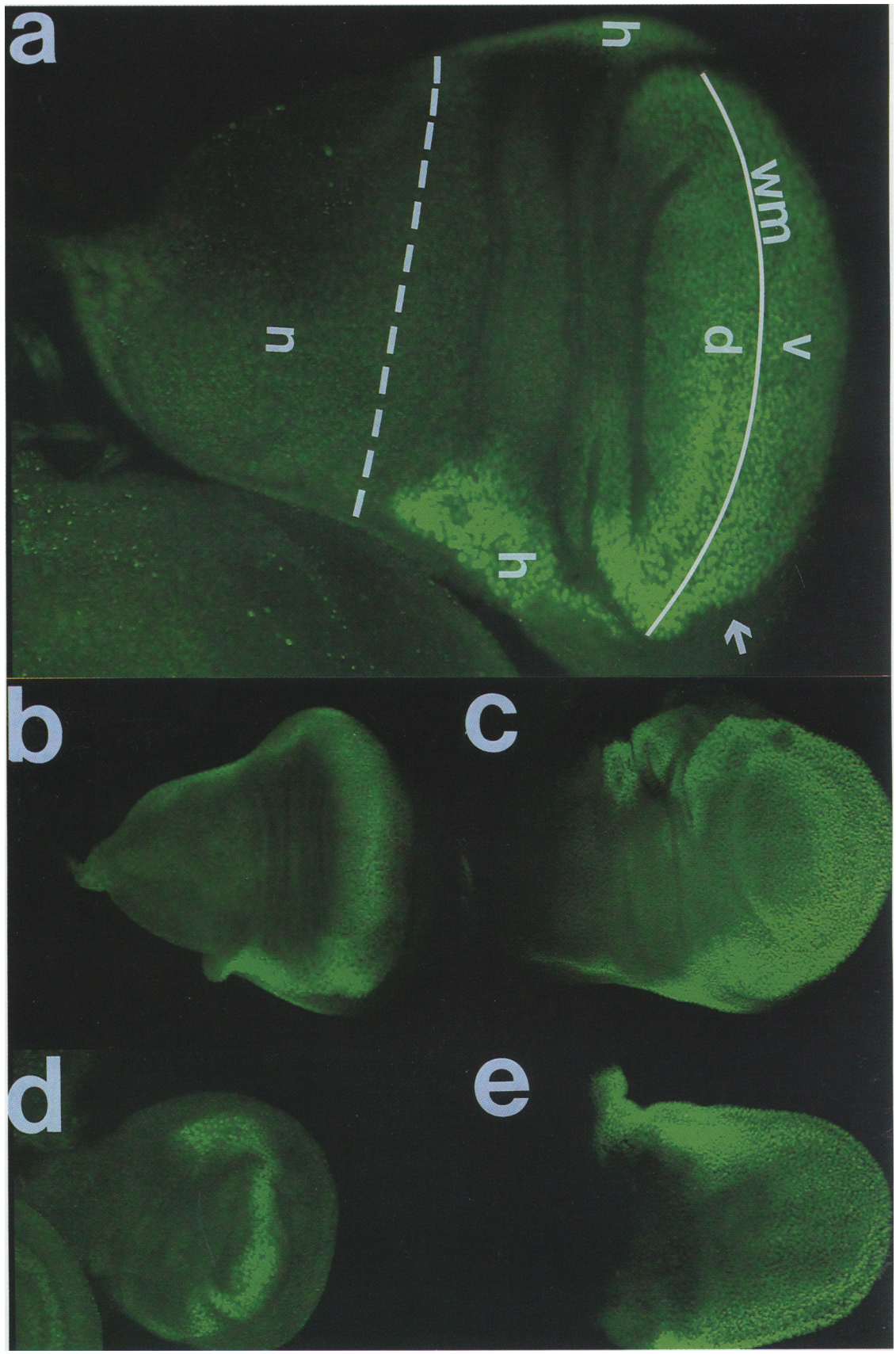

Figure 6. *(See facing page for legend.)*

of expression observed in third-instar discs, limiting elevated *vg* expression to the regions in which *vg* function is required. Thus, a segmentally restricted larval pattern of expression could be imprinted during embryogenesis and interpreted later during larval development. Alternatively, the intronic enhancer may be able to weakly activate *vg* expression (in the correct pattern) without prior embryonic expression but acts synergistically with the low-level expression established during embryogenesis to produce the observed spatially restricted elevated *vg* expression. However, it is possible that the embryonic expression in the wing and haltere primordia is coincidental and not necessary for subsequent expression. P-element-mediated DNA transformation analysis of the putative disc control region (in promoter fusion constructs) should help to elucidate the mechanism by which larval disc expression is activated.

How is vestigial expression initially established in the imaginal disc primordia?

The *Ultrabithorax* (*Ubx*) gene is required to specify haltere imaginal disc development, whereas *Antennapedia* (*Antp*) is required to specify wing disc development. It is not known whether initial establishment of *vg* expression is directly or indirectly responsive to these homeotic genes, because the relevant *vg* control sequences have not been identified. Clearly, other regulators must also exist (e.g., dorsal–ventral patterning genes), as expression is not observed in the mesothoracic and metathoracic leg disc primordia, which also require these homeotic genes for specificity (see Simcox et al. 1991). Because *vg* serves as a molecular marker for the establishment of the wing and haltere primordia, analysis of *vg* expression patterns in genetic backgrounds mutant for potential regulatory genes may identify the genes that specify the identity of these primordia. Furthermore, although the location of sequences required to initially establish *vg* expression in the embryonic disc primordia have not been identified, genetic evidence indicates that all sequences required for wing development reside within the 16-kb interval, including the *vg* transcription unit (Fig. 1, coordinates 0 to + 16; Williams and Bell 1988; J. Williams, unpubl.). P-element-mediated DNA transformation analysis of the interspecifically conserved restriction fragments that we have identified within this region may identify these embryonic control elements, thus allowing a detailed analysis of the mechanism of establishing gene expression in these disc primordia.

What regulatory genes interact with the larval enhancer?

The vg^{83b27} allele is a deletion mutant of intron 2 that abolishes the high level of *vg* expression observed in wing and haltere imaginal discs but does not eliminate expression from the embryonic primordia. Genetic evidence indicates that the intronic element deleted by vg^{83b27} can operate on the *vg* promoter in *cis* or *trans*. Although P-element-mediated DNA transformation experiments will be required to firmly establish the location of this control region, interspecific sequence comparisons have identified a strongly conserved interval within this intron that is a probable candidate for an essential part of this control region. The amplified pattern of *vg* expression in third-instar discs is a broad stripe defining the presumptive wing region of the wing disc and is excluded from presumptive notum cells. Because the notum–wing compartment restriction is established during early larval development (Garcia-Bellido 1975), *vg* may be under the control of developmental regulators involved in establishing or maintaining this restriction. The fact that some vg^{83b27} discs show small parts of the expression pattern (see Fig. 3) indicates that some control sequences may map outside the intronic deletion. This implies that this control element is more complex and suggests that the control region may respond to a number of factors required in establishing this restriction.

vg expression in the wing and haltere discs is essentially a stripe of cells across the distal portion of the disc and is centered on the putative margin region. These patterns suggest that the upstream regulators that activate *vg* expression could also be expressed in similar stripes across the wing and haltere discs at the time *vg* is activated. Such regulators should function during early larval development (first or second instar) to set up amplified *vg* expression. These upstream genes should also be required for wing development (and potentially other pattern formation processes) and may include genes that have already been defined as essential for wing development.

An excellent candidate upstream activator of *vg* is the *wingless* (*wg*) segment polarity gene, which is a component of a signaling pathway required for embryonic and

Figure 6. Expression of the *vg* protein in the presumptive wing and haltere regions of late larval imaginal discs. The *vg* protein expression patterns in wing and haltere discs are shown in *b* and *e*, respectively. (*a*) A highly enlarged photograph of a wing disc. Fate map locations of adult wing disc derivatives (Bryant 1975) are indicated in *a*. Abbreviations: (N) notum; (D) dorsal wing blade; (V) ventral wing blade; (WM) wing margin; (H) wing hinge. The arrow denotes the ventral limit of staining, which precisely demarcates the boundary between the ventral wing blade and the adjacent region of the disc that will form ventral thoracic structures. The region of maximal staining corresponds to the wing margin (solid line), and extends symetrically into the dorsal (D) and ventral (V) wing blade regions of the disc. It appears that most of the presumptive wing blade cells in the disc express *vg*, as *vg* labels essentially all the wing during the early (*c*) and late (*d*) eversion of this structure in the first several hours after puparium formation. The absence of staining in wing imaginal discs isolated from a homozygous protein null fly (data not shown) confirmed that the antibody staining pattern is *vg* specific.

imaginal disc pattern formation (Peifer et al. 1991). *wg* is required during the first- and second-larval instars for wing formation (Baker 1988). Absence of *wg* function results in wing-to-notum transformations, consistent with a role of *wg* in activating genes required in later larval life (i.e., *vg*) to specify wing versus notum development. *wg* mRNA is expressed in a complex pattern in imaginal discs (Baker 1988) but, in the wing disc, is expressed predominantly in a narrow stripe across this disc (and haltere disc), which defines the wing margin (Peifer et al. 1991). The *wg* protein is probably expressed in a broader region flanking this stripe, as *wg* encodes a secreted protein (van den Heuvel et al. 1989). Presumably gene activation is not mediated directly by the *wg* protein but, rather, by a transcription factor that is a nuclear component of the *wg* signaling pathway. Analysis of *vg* imaginal disc expression patterns in genetic backgrounds mutant for *wg* and other potential *trans*-acting regulators of *vg*, and molecular dissection of the *cis*-regulatory elements responsible for its patterned expression in imaginal discs should yield valuable information about the genes required for wing and haltere formation and the proper regulation of *vg* expression during larval development.

Materials and methods

D. melanogaster *stocks and culturing*

Stocks were grown at 24°C and maintained on a synthetic medium (Nash and Bell 1968). The origins, phenotypes, and molecular biology of Df(2R)vg^{136}, Df(2R)vg^{B}, vg^{79d5}, vg^{83b27}, vg^{nw}, and vg^{12} are reported in Williams and Bell (1988) and Williams et al. (1990a), whereas the analysis of In(2R)vg^{W} and its four revertant alleles (vg^{WR1-4}) is described in Williams et al. (1990b). The vg^{nw} and vg^{12} alleles are associated with an exonic deletion (+13 to +16) and an exonic insertion (+2), respectively (for *vg* region coordinates, see Fig. 1). Df(2R)vg^{136} (vg^{136}) has a deletion extending distally from coordinate +17, but it also has an inversion of the +5 to +17 interval. In(2R)vg^{W} (vg^{W}) is a dominant gain-of-function allele associated with an inversion (+1) linking *vg* to the *invected* gene (Williams et al. 1990b). The vg^{WR2-4} alleles are *vg* null derivatives of vg^{W}, which have no *vg* locus alterations (other than the inversion break). Df(2R)vg^{B} is a deletion that includes the entire *vg* locus (Williams and Bell 1988). Oregon-R flies were used as wild type for all studies.

DNA subcloning and sequencing

Culturing and storage of bacteria or λ phage, preparation of DNA, restriction analyses, plaque lifts, and plasmid subcloning were performed according to standard methodology (Maniatis et al. 1982). Genomic *Drosophila* DNA for Southern hybridizations and the genomic library was prepared according to Ish-Horowitz et al. (1979) and repurified by spermine precipitation (Hoopes and McClure 1981). The *D. virilis Sau*3a library was prepared in λ vector EMBL3 as in Williams and Bell (1988). All plasmid subclones were constructed in the Bluescribe plasmid vector (Vector Cloning Systems). Exonuclease III-generated directed deletions for DNA sequencing (Henikoff 1984) were made by utilizing the Erase-a-Base System (Promega). Double-stranded DNA sequencing was performed with ^{35}S-labeled dATP (500 Ci/mmole; New England Nuclear) utilizing T7 DNA polymerase according to the manufacturer's instructions (Pharmacia). To resolve sequence compressions, some constructs were also sequenced with dITP substituted for dGTP.

Sequencing strategies

The sequence of the *vg* cDNAs and corresponding genomic intervals was generated as follows. The longest cDNA is 3.7 kb (cDNA1), containing two *Eco*RI fragments (0.5 and 3.2 kb). The nucleotide sequence of both *Eco*RI fragments was determined, utilizing relevant DNA subclones and exonuclease III-generated, nested deletions. Single-stranded DNA sequence was generated from the +7 *Hin*cII site to the +0.3 *Eco*RI site (see Fig. 1). The sequence of both DNA strands was determined for the remainder of the cDNA *Eco*RI fragments. The cDNA sequence was compared with the genomic DNA sequence derived from relevant genomic subclones or exonuclease III-generated, nested deletions. Single- or double-stranded genomic DNA sequence, including all exonic regions, was generated. This allowed all the exon–intron boundaries to be mapped (shown in Figs. 1 and 4). The splice junctions were also determined from three other independent *vg* cDNAs (cDNAs 2, 3, and 4 from Williams et al. 1990a). Genomic sequences distal to the +16 *Bgl*II site were not sequenced. We believe that no small introns are contained in this region, because the cDNA restriction map is extensive and colinear with the genomic map (Fig. 1). The 3′ end of the cDNA has been mapped previously into this region as well (Williams et al. 1990a). The FastA program was used to search a Swiss protein library (version 18.0) and the tFasta program was used to search the GenBank (release 68.0) and EMBL (release 27.0) nucleotide sequence libraries for protein homology to *vg*.

Filter hybridizations

All gels for Southern hybridization analyses were blotted onto Genescreen Plus membranes using the capillary blot protocol recommended by the manufacturer (Dupont). Hybridization conditions for all plaque lifts and genomic Southern blots were as in Klessig and Berry (1983). High-stringency hybridizations were performed at 42°C; reduced-stringency hybridizations, at 37°C. The initial wash conditions for the melt-off experiments were 0.1× SSC, 0.1% SDS, at 45°C. DNA probes were made from restriction fragments resolved on low-melt agarose gels and oligolabeled by the method of Feinberg and Vogelstein (1983). Probes for the melt-off experiments were generated by nick translation (Maniatis et al. 1982) of the relevant λ clones.

Cloning of the D. virilis vg *locus*

Two overlapping λ clones (V4 and V6), with homology to the *D. melanogaster vg* locus, were isolated from a *D. virilis Sau*3a genomic library (see above). Southern blots of restriction endonuclease digests of λ V4 and V6 DNA were probed with various *D. melanogaster* genomic or cDNA restriction fragments. This allowed the homologous regions to be aligned and indicated that these clones contain *vg* region DNA corresponding to at least the −1 to +18 *D. melanogaster* interval (see Fig. 1). A radiolabeled restriction fragment from the *D. virilis* locus was hybridized under conditions of high stringency to a Southern blot of *Eco*RI restriction-digested *D. melanogaster* and *D. virilis* genomic DNA. No homology was seen in the *D. melanogaster* lane, whereas a single band of the predicted size was detected in the *D. virilis* lane (data not shown). A *D. virilis* restriction fragment homologous to exon 4 was cloned, sequenced, and aligned with the *D. melanogaster* exon 4 sequence. Strong conservation of the protein product of this exon was observed (Fig. 5a). Collec-

tively, these results indicate that we have cloned the *D. virilis* *vg* locus and that this locus is single copy. The overall size and organization of the locus is similar in both species, whereas the colinearity of homologous regions indicates that no significant sequence rearrangement within the locus has occurred since these species diverged (data not shown).

Identification of interspecifically conserved regions

Southern blots of restriction endonuclease-digested *D. melanogaster* plasmid DNA subclones, spanning the entire *vg* locus, were hybridized and washed under reduced stringency conditions to nick-translated *D. virilis* V4 and V6 λ clones. The resultant blots were washed at increasing stringency (in increments of 5°) until all of the probe was melted from the filter. The filters were autoradiographed after each wash to monitor the removal of the probe. The blots were then rehybridized and washed sequentially as above with a nick-translated full-length *D. melanogaster* cDNA (cDNA 1 in λ GT10) and, finally, with a labeled EMBL3 λ clone containing genomic DNA spanning the entire *D. melanogaster* *vg* locus (λ 64 from Williams and Bell 1988). The results from the *D. melanogaster* cDNA and genomic DNA melt-offs allowed us to determine the melting point of homologous DNA hybrids, including the *D. melanogaster* exons alone or the entire restriction fragments, respectively. This will vary, as GC-rich regions show higher thermal stability than AT-rich regions. Interspecific hybridization (strong or weak) was observed with restriction fragments from throughout the *D. melanogaster* locus. Most of this hybridization signal washed off at ~10–20° lower than the equivalent intraspecific DNA hybrids. These results are indicative of an average sequence divergence of 10–20% (Bonner et al. 1973). However, some interspecific DNA hybrids denatured at higher temperatures, indicating patches of near perfect conservation within these fragments. This indicates that most of the *vg* locus contains some conserved sequences, as nonessential sequences are highly diverged between these species (Blackman and Meselson 1986; Kassis et al. 1986). However, several strongly hybridizing regions were detected, indicating that some regions of the locus are extensively interspecifically conserved (shown in Fig. 1).

Antibody production

Two *vg* cDNA3 (Williams et al. 1990a) fragments were cloned into the *Bam*HI site of the T7 expression vector Pet3c (Studier et al. 1990). One is an in-frame fusion that expresses the carboxy-terminal 328 amino acids of the *vg* ORF (*vg*-1), whereas the second (*vg*-2) is a smaller fusion protein containing the carboxy-terminal 179 amino acids (see Fig. 5). Both proteins contain the first 13 amino acids encoded in the vector. The recombinant proteins were partially purified from insoluble inclusion bodies, and *vg*-1 protein was injected into rabbits (1 mg each) after emulsification with Freund's complete adjuvant and boosted at 2-week intervals with antigen emulsified with Freund's incomplete adjuvant. Antibodies were affinity purified by passage over either a *vg*-1 or a *vg*-2 antigen column and eluted with 4 M guanidine-HCl in PBS. After extensive dialysis against PBS, the purified antibody was passed over an *Escherichia coli*-soluble protein column to remove cross-reactive and "sticky" antibodies. The flowthrough antibody was quantified by UV absorption and stored at 4°C after the addition of NaN_3 to 0.02% (wt/vol). The *vg* antigen and *E. coli*-soluble protein columns were prepared by coupling the protein to Actigel resin, according to the manufacturer's instructions (Sterogene). Antibodies purified on the *vg*-1 column gave much higher nonspecific background staining in embryos and imaginal discs than *vg*-2 affinity-purified antibodies. This is presumably due to the fact that the *vg*-1 protein contains several repetitive protein motifs (i.e., homopolymeric glycine runs and two *paired* repeats), and antibodies to epitopes in these regions may cross-react with other *Drosophila* proteins. All *vg* antibody staining reported here was performed with antibodies from a 6-month bleed that were affinity purified against a *vg*-2 column.

Histochemistry

Antibody staining of imaginal discs was performed as described previously (Skeath and Carroll 1991). Briefly, dissected disc complexes were incubated with *vg* antibodies (0.5–1 μg/ml), washed, and incubated with biotinylated goat anti-rabbit IgG (Vector), washed, and incubated with fluorescein-conjugated streptavidin. Double-fluorescence labeling of imaginal discs from a nuclear-localized β-galactosidase-expressing enhancer trap line (ubiquitously staining in imaginal discs; N. Brown, pers. comm.) with anti-*vg* and anti-β-galactosidase antibodies confirmed that the *vg* protein is nuclear localized. For this double labeling with β-galactosidase, a β-galactosidase-specific monoclonal antibody (Boehringer Mannheim) was detected with rat anti-mouse IgG, followed by rhodamine-conjugated goat anti-rat IgG antibodies. Microscopy was on a Zeiss/IM35 equipped with a Bio-Rad MRC600 Lasersharp Confocal system. Digoxygenin in situ hybridizations to embryos and discs were performed by modification of the procedure of Tautz and Pfiefle (1989). The differences were that (1) the embryos were treated with proteinase K for 12 min; (2) after washing hybridized embryos twice for 20 min with PBS containing 0.1% Tween 20 (vol/vol), two additional washes for 20-min at room temperature with PBS containing 0.1% BSA, 2% Triton X-100, were included, and antibody incubations (1 hr) and washing were performed at room temperature in this buffer; (3) color development was allowed to proceed overnight for embryos; and (4) after stopping the color reaction, embryos were mounted for at least 1 hr in 50 mM Tris(8.8) 10% glycerol, whereas discs were mounted in 50 mM Tris (8.8) 70% glycerol. Probes were prepared by oligolabeling (Feinberg and Vogelstein 1983) or polymerase chain reaction (PCR) runoff (see below). Three *vg* cDNA fragments were used as probes. From 5′ to 3′, these were an *Eco*RI–*Hin*cII untranslated leader containing probe (probe A); a coding region-specific fragment, corresponding to the *vg*-2 expression vector insert (probe B; see Fig. 5); an untranslated trailer-specific probe from the *Bgl*II site to the 3′ end of cDNA1 (probe C; see Fig. 1). All three probes recognized identical expression patterns in embryos and imaginal discs (data not shown). The same pattern was also recognized with strand-specific antisense probes generated by PCR runoff (Fleming et al. 1990) of a probe A-containing construct (data not shown). Thus, the reported expression pattern is *vg* specific, as it is identified by an antisense probe and recognized by probes from the untranslated leader, coding region, and untranslated trailer. The embryonic expression patterns shown in Figure 2 were from embryos hybridized with oligolabeled probe A, whereas the imaginal disc patterns in Figure 3 were identified with PCR runoff-generated antisense probe A. Microscopy was performed with bright-field optics using a Zeiss Axiophot.

Acknowledgments

We thank James Skeath for technical advice and assistance and many thoughtful discussions; Steve Paddock for his extensive help with confocal microscopy; Bruce Thalley and Nadean Brown for technical advice, and Alfonso Martinez-Arias for

communication of results prior to publication. We acknowledge Tom Griggliatti, in whose laboratory some of the molecular biology was performed. We especially thank John Tamkun, Teresa Orenic, and James Skeath for their critical reviews of the manuscript. This work was supported by National Sciences and Engineering Research Council grants (NSERC) to J.B.B. (A9704), NSERC and Killam postdoctoral fellowships to J.A.W., and the Howard Hughes Medical Institute.

The publication costs of this article were defrayed in part by payment of page charges. This article must therefore be hereby marked "advertisement" in accordance with 18 USC section 1734 solely to indicate this fact.

References

Akam, M. 1987. The molecular basis for metameric pattern in the *Drosophila* embryo. *Development* **101:** 1–22.

Alexandrov, I.D. and M.V. Alexandrova. 1987. A new nw allele and interallelic complementation at the *vg* locus of *Drosophila melanogaster*. *Drosophila Inf. Serv.* **66:** 11.

Baker, N.E. 1988. Embryonic and imaginal requirements for *wingless*, a segment-polarity gene in *Drosophila*. *Dev. Biol.* **125:** 96–108.

Bate, M. and A. Martinez-Arias. 1991. The embryonic origin of imaginal discs in *Drosophila*. *Development* **112:** 755–761.

Beverley, S.M. and A.C. Wilson. 1984. Molecular evolution in *Drosophila* and the higher *diptera* II. A time scale for fly evolution. *J. Mol. Evol.* **21:** 1–13.

Blackman, R.K. and M. Meselson. 1986. Interspecific nucleotide sequence comparisons used to identify regulatory and structural features of the *Drosophila hsp82* gene. *J. Mol. Biol.* **188:** 499–515.

Bonner, T.L., D.T. Brenner, B.R. Neufeld, and R.J. Britten. 1973. Reduction in the rate of DNA reassociation by sequence divergence. *J. Mol. Biol.* **81:** 123–135.

Bownes, M. and S. Roberts. 1981. Regulative properties of wing discs from the *vestigial* mutant of *Drosophila melanogaster*. *Differentiation* **18:** 89–96.

Bryant, P.J. 1975. Pattern formation in the imaginal wing disc of *Drosophila melanogaster*: Fate map, regeneration and duplication. *J. Exp. Zool.* **193:** 47–78.

Bryant, S.V., V. French, and P.J. Bryant. 1981. Distal regeneration and symmetry. *Science* **212:** 993–1002.

Burtis, K.C., C.S. Thummel, C. Weldon Jones, F.D. Karim, and D.S. Hogness. 1990. The *Drosophila* 74EF early puff contains *E74*, a complex ecdysone-inducible gene that encodes two *ets*-related proteins. *Cell* **61:** 85–99.

Campos-Ortega, J.A. and V. Hartenstein. 1985. *The embryonic development of* Drosophila melanogaster. Springer-Verlag, Berlin.

Cavener, D.R. 1987. Comparison of the consensus sequence flanking translational start sites in *Drosophila* and vertebrates. *Nucleic Acids Res.* **15:** 1353–1361.

Cohen, S.M. 1990. Specifications of limb development in the *Drosophila* embryo by positional cues from segmentation genes. *Nature* **343:** 173–177.

Cohen, B., E.A. Wimmer, and S.M. Cohen. 1991. Early development of leg and wing primordia in the *Drosophila* embryo. *Mech. Dev.* **33:** 229–240.

Cronmiller, C., P. Schedl, and T.W. Cline. 1988. Molecular characterization of *daughterless*, a *Drosophila* sex determination gene with multiple roles in development. *Genes & Dev.* **2:** 1666–1676.

Feinberg, A.P. and B. Vogelstein. 1983. A technique for radiolabeling DNA restriction endonuclease fragments to high specific activity. *Anal. Biochem.* **132:** 6–13.

Fleming, R.J., T.N. Scottgale, R.J. Diederich, and S. Artavanis-Tsakonas. 1990. The gene *Serrate* encodes a putative EGF-like transmembrane protein essential for proper ectodermal development in *Drosophila melanogaster*. *Genes & Dev.* **4:** 2188–2201.

Frigerio, G., M. Burri, D. Bopp, S. Baumgartner, and M. Noll. 1986. Structure of the segmentation gene *paired* and the *Drosophila PRD* gene set as part of a gene network. *Cell* **47:** 735–746.

Fristrom, D. 1969. Cellular degeneration in the production of some mutant phenotypes in *Drosophila melanogaster*. *Mol. Gen. Genet.* **103:** 363–379.

Garcia-Bellido, A. 1975. Genetic control of wing disc development in *Drosophila*. Ciba Symp. **29:** 161–182.

Haynes, S.R., B.A. Mozer, N. Bhatia-Dey, and I.B. Dawid. 1989. The *Drosophila fsh* locus, a maternal effect homeotic gene, encodes apparent membrane proteins. *Dev. Biol.* **134:** 246–257.

Henikoff, S. 1984. Unidirectional digestion with exonuclease III creates targeted breakpoints for DNA sequencing. *Gene* **28:** 351–359.

Hoopes, B.C. and W.R. McClure. 1981. Studies on the selectivity of DNA precipitation by spermine. *Nucleic Acids Res.* **9:** 5493–5505.

Ingham, P.W. 1988. The molecular genetics of embryonic pattern formation in *Drosophila*. *Nature* **335:** 25–34.

Ish-Horowicz, D., S.M. Pinchin, P. Schedl, S. Artavanis-Tsakonas, and M. Mirault. 1979. Genetic and molecular analysis of the 87A7 and 87C1 heat inducible loci of *D. melanogaster*. *Cell* **18:** 1351–1358.

James, A.A. and P. Bryant. 1981. Mutations causing pattern deficiencies and duplications in the imaginal wing disc of *Drosophila melanogaster*. *Dev. Biol.* **85:** 39–54.

Kassis, J.A., S.J. Poole, D.K. Wright, and P.H. O'Farrell. 1986. Sequence conservation in the protein coding and intron regions of the *engrailed* transcription unit. *EMBO J.* **5:** 3583–3589.

Klessig, D. and J.O. Berry. 1983. Improved filter hybridization method for detection of single copy sequences in large eukaryotic genomes. *Plant Mol. Biol. Rep.* **1:** 12–18.

Lewis, E.B. 1954. The theory and application of a new method of detecting chromosomal rearrangements in *Drosophila melanogaster*. *Am. Nat.* **88:** 225–239.

Lindsley, D.L. and E.H. Grell. 1968. Genetic variations of *Drosophila melanogaster*. *Carnegie Inst. Washington Publ.* **627.**

Madhavan, M.M. and H.A. Schneiderman. 1977. Histological analysis of the dynamics of growth of imaginal discs and histoblast nests during the larval development of *Drosophila melanogaster*. *Wilhelm Roux's Arch. Dev. Biol.* **183:** 269–305.

Maniatis, T., E.F. Fritsch, and J. Sambrook. 1982. *Molecular cloning: A laboratory manual*. Cold Spring Harbor Laboratory, Cold Spring Harbor, New York.

Nash, D. and J.B. Bell. 1968. Larval age and the pattern of DNA synthesis in polytene chromosomes. *Can. J. Genet. Cytol.* **10:** 82–92.

Pearson, W.R. and D.J. Lipman. 1988. Improved tools for biological sequence comparison. *Proc. Natl. Acad. Sci.* **85:** 2444–2448.

Peifer, M., C. Rauskolb, M. Williams, B. Riggleman, and E. Wieschaus. 1991. The segment polarity gene *armadillo* interacts with the *wingless* signaling pathway in both embryonic and adult pattern formation. *Development* **111:** 1029–1043.

Rabinow, L. and J.A. Birchler. 1990. Interactions of *vestigial* and

scabrous with the *Notch* locus of *Drosophila melanogaster*. *Genetics* **125:** 41–50.

Regulski, M., N. McGinnis, R. Chadwick, and W. McGinnis. 1987. Developmental and molecular analysis of *Deformed*; a homeotic gene controlling *Drosophila* head development. *EMBO J.* **6:** 767–777.

Scott, M.P. and S.B. Carroll, 1987. The segmentation and homeotic gene network in early *Drosophila* development. *Cell* **51:** 689–698.

Shaw, G. and R. Kamen. 1986. A conserved AU sequence from the 3′ untranslated region of GM-CSF mRNA mediates selective mRNA degradation. *Cell* **46:** 659–667.

Simcox, A.A., E. Hersperger, A. Shearn, R.S. Whittle, and S.M. Cohen. 1991. Establishment of imaginal discs and histoblast nests in *Drosophila*. *Mech. Dev.* **34:** 11–20.

Skeath, J.B. and S.B. Carroll. 1991. Regulation of *achaete-scute* gene expression and sensory organ pattern formation in the *Drosophila* wing. *Genes & Dev.* **5:** 984–995.

Stanley, W.F. 1931. The effect of temperature on *vestigial* wing in *Drosophila melanogaster*, with temperature-effective periods. *Physiol. Zool.* **IV:** 394–400.

Studier, F.W., A.H. Rosenberg, and J.J. Dunn. 1990. Use of T7 RNA polymerase to direct the expression of cloned genes. *Methods Enzymol.* **185:** 60–89.

Tautz, D. and C. Pfeifle. 1989. A non-radioactive in situ hybridization method for the localization of specific RNAs in *Drosophila* embryos reveals translational control of the segmentation gene *hunchback*. *Chromosoma* **98:** 81–85.

van der Heuvel, M., R. Nusse, P. Johnston, and P.A. Lawrence. 1989. Distribution of the *wingless* gene product in *Drosophila* embryos: A protein involved in cell-cell communication. *Cell* **59:** 739–749.

Whittle, J.R.S. 1990. Pattern formation in imaginal discs. *Sem. Cell Biol.* **1:** 241–252.

Wieschaus, E. and W.J. Gehring. 1976a. Gynandromorph analysis of the thoracic disc primordia in *Drosophila melanogaster*. *Wilhelm Roux's Arch. Dev. Biol.* **180:** 31–46.

———. 1976b. Clonal analysis of primordial disc cells in the early embryo of *Drosophila melanogaster*. *Dev. Biol.* **50:** 249–263.

Wilde, C.D. and M. Akam. 1987. Conserved sequence elements in the 5′ region of the *Ultrabithorax* transcription unit. *EMBO J.* **6:** 1393–1401.

Wilkins, A.S. and D. Gubb. 1991. Pattern formation in the embryo and imaginal discs of *Drosophila*: What are the links? *Dev. Biol.* **145:** 1–12.

Williams, J. and J.B. Bell. 1988. Molecular organization of the *vestigial* region in *Drosophila melanogaster*. *EMBO J.* **7:** 1355–1363.

Williams, J., A.L. Atkin, and J.B. Bell. 1990a. The functional organization of the *vestigial* locus in *Drosophila melanogaster*. *Mol. Gen. Genet.* **221:** 8–16.

Williams, J., I.M. Scott, A.L. Atkin, W.J. Brook, M.A. Russell, and J.B. Bell. 1990b. Genetic and molecular analysis of vg^{U} and vg^{W}: Two dominant *vg* alleles associated with gene fusions in *Drosophila*. *Genetics* **125:** 833–844.